

Smallest Of-Order Statistic-CFAR Analysis in Weibull Clutter

M.Sc. Salih M. Salih⁽¹⁾, Dr. Ali Y. Fattah⁽²⁾ & Dr. Bayan M. Sabbar⁽³⁾

Received on:13/3 /2005

Accepted on:8 12 /2005

Abstract

The performance of Cell Averaging-Constant False Alarm Rate (CA-CFAR) degrades rapidly in nonideal conditions caused by the presence of a strong target signal in one of the reference cells. The Order Statistic-CFAR (OS-CFAR) is used to eliminate the reference cells with a strong input. The performance of the Smallest Of -Order Statistic (SO-OS) detector is evaluated to determine the signal-to-clutter ratio required achieving a particular probability of detection in clutter environments whose amplitude statistics are modeled by the Weibull distribution, and where the clutter dominates receiver noise. The performance is evaluated in both homogeneous and nonhomogeneous clutter. The analysis shows that the SO-OS detector is quite robust against both the interference and multiple target situations.

تحليل مرتب الخواص - الأصغر من - لمعدل الإنذار الخطأ الثابت بجلية ويبل

الخلاصة

إن أداء متوسط الخلايا - لمعدل الإنذار الخطأ الثابت يقل بشكل سريع تحت تأثير الضوضاء الغير مثالية المتمثلة بوجود أهداف عديدة بإحدى مجموعتي خلايا التخمين. إن مرتب الخواص - لمعدل الإنذار الخطأ الثابت يتم استخدامه لغرض إلغاء خلايا التخمين ذات القدرة العالية. إن أداء معالج الأصغر من - لمرتب الخواص تم تقييمه لغرض تحديد نسبة الإشارة - إلى - الضوضاء اللازمة للإعطاء احتمالية الكشف المطلوبة عندما تكون الجلبة موزعة توزيع ويبل، ومسيطرة كلياً على إشارة الضوضاء المستلمة. تقييم أداء المعالج تم تحت تأثير ظروف جلبة متجانسة وغير متجانسة. التحليل بين إن معالج الأصغر من - لمرتب الخواص ذو متانة عالية ضد التثويش وتعدد الأهداف بخلايا التخمين.

Abbreviations and Symbols

ADT	Average Detection Threshold
CFAR	Constant False Alarm Rate
CA-CFAR	Cell Averaging-Constant False Alarm Rate
CDF	Cumulative Distribution Function
GO-OS	Greatest Of-Order Statistic
OS-CFAR	Order Statistic-Constant False Alarm Rate
SO-OS	Smallest Of-Order Statistic
M	Number of Estimation Cells
P_d	Probability of Detection

(1) Electrical Eng. Dept., College of Eng., University of Al-Anbar, Iraq

(2) Electrical and Electronic Eng. Dept., University of Technology, Baghdad/Iraq

(3) Electrical Eng. Dept., University of Al-Mustansiriyah, Baghdad/Iraq

P_{fa}	Probability of False Alarm
R	Number of Cells in Clutter
$R1$	Leading Interfering Targets
$R2$	Lagging Interfering Targets
b	Weibull Skewness Parameter
α	Threshold Multiplier That Determine the Probability of False Alarm
γ	Scale Parameter
μ	Average Noise Power
μ_i	Average Thermal Noise Power
μ_c	Average Clutter Power
$Q_{E,L}(x)$	Cumulative Distribution Function for Early and Late Estimation Cells
$Q_w(x)$	Cumulative Distribution Function of Weibull Distribution
$P_w(x)$	Probability Density Function of Weibull Distribution
\overline{SNR}	Average Signal-To-Noise Ratio

1. Introduction

A target is detected when the output of the radar receiver crosses a predetermined fixed threshold level set to achieve a specified probability of false alarm. In many situations, however, the clutter echoes and or hostile noise can be much greater than receiver internal noise. When this happens, the receiver threshold can be exceeded and many false alarms can occur. In many applications where the noise can change due to interference or varying clutter. The solution is an *Adaptive Threshold* adjustment, designed to keep the false-alarm probability constant despite changes in the background noise or interference. Many techniques can yield Constant False Alarm Rate (CFAR), under specific restrictions. CFAR usually reduces the probability of detection compared to similar case at known and stable noise level. In a Cell-Averaging (CA-CFAR) system the threshold

adjustment for a specified resolution cell is based on the average detected input from the neighboring cells during the same pulse or scans. This method works well when the background interference is statistically homogeneous over the range. This assumption is violated in two major situations [1]:

- When the reference cells cross an edge in the clutter background.
- When one or more reference cells include returns from other targets.

When the cell under test is in the clear side of the edge, in the original CA-CFAR, the reference cells in the clutter will unnecessarily increase the threshold, causing a decrease in the probability of detection. The Greatest Of-CFAR (GO-CFAR) strategy will worsen the problem. One solution here is to use the opposite strategy by selecting the lower of the two levels. This type is known as the "*Smallest Of-CFAR*" or *SO-CFAR*. The presence of

a strong target signal in one of the reference cells is similar to the problem of having stronger clutter in several adjacent reference cells. The SO-CFAR is rather wasteful when applied to problem (b). The SO-CFAR can fail when there are two interfering targets, in two reference cells on the two sides of the cell under test. In conclusion, the SO-CFAR is a simple but wasteful solution to Greatest Of (GO) the problem of a single interfering target and a doubtful solution to the problem of two or more interfering targets.

Several other solutions to the problem of maintaining CFAR in multiple-target situations have been proposed. They yield better Performance but require more complex implementation. Rohling [1] suggested a different approach to the elimination of reference cells with a strong input. This is called Order Statistic-Constant False Alarm Rate (OS-CFAR).

Several nonlinear estimation techniques have been proposed to reduce the above problems. The nonlinearity may involve taking the the average of the two groups, the Smallest Of (SO) the average of the two groups, and variations on these recent interest has also concentrated on order statistic (OS) detectors that use the K th largest on M range cells

Order Statistics characterize amplitude information by ranking observations in which differently ranked outputs can estimate statistical properties of the distribution from which they stem. The order statistic corresponding to a rank K is found by taking the set of M observations $X(k)$,

$k=1,2,\dots,M$, and ordering them with respect to increasing magnitude.(i.e. $x_1 \leq x_2 \leq x_3 \leq x_4 \leq \dots \leq x_M$) [2, 3, 4], the K th largest samples taken as an estimate for the unknown noise level.

The GO-OS detector has the best detection performance at clutter edges; its performance degrades at multiple target situations. The SO-OS detector introduces a best detection performance than simple CA-CFAR family, conventional OS-CFAR and the GO-OS detector. Most papers are limited to Rayleigh distributed receiver noise. Real world clutter statistics are generally not Rayleigh distributed so, the performance of the above algorithm can be substantially degraded. The model uses a Weibull distribution to model the clutter. The approximation technique is applied here to study the performance of the SO-OS detector under uniform and nonuniform background distribution. The block diagram of the SO-OS processor is shown in fig. (1)

2. Mathematical Model

The processor is assumed to use an approximation of the magnitude, where I and Q are "In-phase" and "Quadrature" channels, respectively [5, 6] of the sampler that follows the matched filter to determine the threshold. A variety of probability density functions may be used to model this amplitude. The Cumulative Distribution Function (CDF) of the Weibull distribution $Q_w(x)$ is given by [6, 8]:

$$Q_w(x) = 1 - \exp\left(-x^b/\gamma\right), \quad x \geq 0 \quad (1)$$

Where b is the skewness parameter of the distribution and γ is the scale parameter, where both are greater than zero. At $b=2$ the distribution reduces to the Rayleigh distribution. Smaller values of b increase the skewness of the distribution, and allow the simulation of the *spiky* clutter. The probability density function of the Weibull distribution is the derivative of the CDF with respect to x [6, 7, 8]:

$$P_w(x) = \frac{d}{dx} Q_w(x) = \frac{b}{\gamma} x^{b-1} \exp\left(-\frac{x^b}{\gamma}\right), x \geq 0 \quad (2)$$

The probability density functions in Fig. (1) $P_{SO}(x)$ Refers to the density function at the output of the selection logic of the order statistic calculator for SO detector, similar notation for the cumulative distribution function ($Q_{SO}(x)$). The threshold multiplier α required guaranteeing a particular P_{fa} is determined as follows.

Since the threshold is modeled as a random variable, the P_{fa} is given by [1, 6, 8]: $P_{fa} = \int_0^{\infty} Q_T(x) P_T(x) dx \quad (3)$

The cumulative distributions at the OS calculator output is given by [1, 6, 8]

$$Q_{L,E}(x) = \sum_{i=k}^M \binom{M}{i} [Q_w(x)]^i [1 - Q_w(x)]^{M-i} \quad (4)$$

In the SO-OS detector, the noise power is the smaller of the order statistic E and L estimation cells

respectively, the CDF of this processor is given by [6, 9]:

$$Q_{SO}(x) = Q_E(x) + Q_L(x) - Q_E(x)Q_L(x) \quad (5)$$

And the cumulative distribution at the output of the multiplier is

$$Q_T(x) = Q_E\left(\frac{x}{\alpha}\right) + Q_L\left(\frac{x}{\alpha}\right) - Q_E\left(\frac{x}{\alpha}\right)Q_L\left(\frac{x}{\alpha}\right) \quad (6)$$

Eqs. (3) and (6) are used to calculate the values of the threshold multiplier α that gives a particular P_{fa} , for equivalent distribution in both sets of estimation cells ($Q_E(x) = Q_L(x)$).

3. ADT Algorithm

The *Average Detection Threshold (ADT)* adopted here to evaluate the threshold algorithm, when square-law detection is used; is defined as [6, 8].

$$ADT = \frac{\alpha S^2}{\mu}$$

Where αS^2 represents the required signal energy to achieve a particular P_d , μ is the average noise power and ADT represents a required SNR.

The second moment of the output of the selection logic is used to obtain the ADT. The threshold multiplier α is squared when the squaring device is included [6,8], the ADT is then obtained from

$$\frac{1}{\mu} \alpha^2 S^2 \quad (7)$$

Using the first derivative of $Q_{SO}(x)$ for the specific detector, this is given by [6, 8]:

$$ADT = \frac{\alpha}{\mu} \int_0^{\infty} x^2 \left[\frac{d}{dx} (Q_{SO}(x)) \right] dx \tag{8}$$

The probability density function of the detector out of the SO calculator can be obtained by differentiating Eq. (5) with respect to x, which yields:

$$P_{SO}(x) = \frac{d}{dx} Q_{SO}(x) = P_E(x) + P_L(x) - [P_E(x) \cdot Q_L(x) + P_L(x) \cdot Q_E(x)] \tag{9}$$

Since the random variables at the input to the OS calculators are assumed independent and identically distributed, the density function at the output is obtained by differentiating Eq. (4) with respect to x [1].

$$P_{E,L}(x) = \frac{d}{dx} (Q_{E,L}(x)) = K \binom{M}{K} [1 - Q_W(x)]^{M-K} \times [Q_W(x)]^{K-1} P_W(x) \tag{10}$$

The mean noise energy is given by [6]:

$$\mu = \int_0^{\infty} \frac{b}{\gamma} x^{b+1} \exp\left(-\frac{x^b}{\gamma}\right) dx \tag{11}$$

Eqs. (4), (10), and (11) are substituted into Eq. (8) to calculate the value of ADT for a particular value of α , which was previously calculated at different values of the skewness parameter b, and the result formula is:

$$ADT = \frac{\alpha}{\int_0^{\infty} \frac{b}{\gamma} x^{b+1} \exp\left(-\frac{x^b}{\gamma}\right) dx} \int_0^{\infty} x^2 \cdot \left[K \binom{M}{K} \cdot [1 - Q_W(x)]^{M-K} \cdot [Q_W(x)]^{K-1} \cdot P_W(x) \right] dx$$

4. Interference in an Estimation Cells

The detection analysis of this processor is extended to the case where

the interference exists within the estimation cells. If the interference is large, one or more of the cells used for background clutter estimation cells is well above the average value of the remaining cells. This interference could be caused by multiple aircraft flying information, or by jamming. The earlier analysis must be modified to evaluate the performance of a threshold algorithm when the amplitudes of one or more of the cells are represented by different density functions. If the interference is assumed to generate a constant return, this density function describes a constant signal in Weibull-distributed background noise.

To avoid evaluating the Weibull-plus-signal distribution functions, it is convenient to assume that the mean interference is much greater than the clutter in the remaining estimation cells. This approximation becomes more accurate as the returned energy from the interference increases relative to the energy in the remaining estimation cells. Then reducing M in the Eqs. (4), and (10) by one approximates the density function of the detector.

If one of the cells contains interference, the calculation is modified as follows. The P_{fa} is still given by Eq. (3) with $Q_E(x) = Q_L(x)$. That is, the threshold multiplier is set with no interference present. As in the noninterference case, Eq. (3) is solved for α , given a desired P_{fa} . The ADT is obtained from Eq. (8), using Eqs. (4), and (10) with $Q_E(x)$ and $P_E(x)$ as a function of M-1 estimation cells. Note that the actual cell occupied by the

interference is irrelevant to this analysis.

5. Clutter Boundaries Analysis

The reference channel is always assumed to be homogeneous and representative of the primary target distribution under the null hypotheses.

However, the real world clutter background is not identically distributed among the estimation cells. This nonhomogeneity in the background environment occurs when one or more of these cells contain additional energy either from multiple targets or from intentional jamming.

The clutter boundary is modeled as a step function discontinuity in noise power. The window of size M , it is assume that there are R cells coming from heavy clutter region each with power level $\mu_c(\mu_c = \mu(1 + CNR))$ [9, 10], where CNR denotes the clutter-to-thermal noise ratio, and the remaining $M-R$ cells having thermal noise only with power level $\mu_i(\mu_i = \mu)$ each. The observations in both cases are assumed to be statistically independent. Then, the CDF of the K th ranked cell has a form given by [7, 12];

$$Q_{E,L}(x) = \sum_{j=K}^M \sum_{i=\max(0, M-j)}^{\min(j, M-R)} \binom{M-R}{j}^i [Q_1(x)]^j \times [1-Q_1(x)]^{M-R-j} \binom{R}{j-i} [Q_2(x)]^{i-j} [1-Q_2(x)]^{R-i+j} \tag{12}$$

$Q_1(x)$ and $Q_2(x)$ denote the $CDFs$ of the Rayleigh and Weibull distributed

receiver noise of the reference cells respectively.

Equation (12) can now be substituted into Eq.(3) to obtain the P_{fa} at clutter boundaries. The threshold Multiplier α is adjusted using Eq. (4) with $Q_E(x) = Q_L(x)$ to yield a particular P_{fa} in Rayleigh-distributed receiver noise for the selected OS cell. Next, a clutter "front" is passed through the estimation cells. These fronts consist of Weibull-distributed clutter having a variance (20 dB for example) above that used to initially set the threshold. The front advances one estimation cell at a time until it covers all the cells. For the first M cells that the front covers, the target test cell remains in Rayleigh-distributed receiver noise. After that, the test cell is assumed to respond to Weibull-distributed clutter. Thus, a substantial performance change occurs when the front crosses the M th estimation cell.

The background energy μ in Eq. (8) has one of two values, depending on whether or not the test cell responds to clutter.

6. Simulation Results

6.1 Threshold Multiplier Amplitude

To determine the threshold multiplier amplitude (α), it is convenient to normalize W so that it has unity mean, then γ in Eq. (1) can be set to unity [6]. The threshold multiplier α is determined under the hypothesis that

the noise alone is present in the reference channel. The value of α for SO-OS detector is numerically computed by solving Eq. (3) with Eq. (6). In all numerical results, the window size M is 24 cells and two values of P_{fa} are assumed: 10^{-4} (solid line) and 10^{-6} (dashed line).

It can be seen that From Fig.(2), the threshold multiplier α decreases as the order statistic cell K increases. As the skewness of the Weibull distribution increases (i.e. as b decreases), the threshold multiplier values (α) increases, raising the threshold to account for noise spikes.

6.2 Average Detection Threshold Calculation

The ADT is now calculated for the detector. Eq. (8) with (9) is used to calculate the ADT for this detector. The ADT is obtained from these equations with $Q_E(x)$ and $P_E(x)$ as a function of $(M-1)$ estimation cells for single interference case. The threshold multiplier is set with no interference present in the reference cells, and its values are obtained by solving Eq. (3), which was previously calculated for the design values of P_{fa} (10^{-4} and 10^{-6}), and different skewness parameter b . Fig. (3a) is plotted at $P_{fa}=10^{-4}$.

In the four pairs (b) that end at $M=23$ represents the single interference case, with interference case the best performance (i.e. smallest ADT) occurs near $K=20$. With no interference case, the best performance occurs also near $K=20$. For this detector a relatively

wide performance plateau exists for K between 16 and 22 for the Rayleigh amplitude ($b=2$) case within which the ADT varies less than 0.2 dB, the width of this plateau decreases for more spiky clutter. The detector introduces a lower loss in case of single interference. The higher loss occurs at higher values of K for this detector, so, the smaller values of K can accommodate many interference-dominated clutter estimation cells in *Rayleigh* clutter, and this option becomes less attractive as the clutter becomes spikier. The interference causes a performance loss of only 1 dB or less for $b \geq 1$ and $K=20$. The performance is degraded by about 19 dB as b varies from Rayleigh to Weibull with $b=0.5$.

Fig. (3b) is plotted for $P_{fa}=10^{-6}$, the same results approximately are obtained. The ADTs are all higher and more degradation is caused by the interference (additional CFAR loss).

6.3 Order Statistic Cell (K)

The threshold multiplier α is calculated to guarantee $P_{fa}=10^{-4}$ at a value of $b=1.5$. The representative rank K , which makes P_{fa} insensitive to uncertainty in the clutter distribution model, is taken as an even number (for example). Then Eq. (3) is used to calculate the P_{fd} at different values of b . Figs. (4) shows these results for the detector.

From this figure, $K=24$ (i.e., the maximum value of M) shows the least sensitivity to changes in b , while $K=8$ shows the most sensitivity for SO-OS

detector. Similar results are obtained when the threshold is adjusted with $0.5 \leq b \leq 2$. Also, the same results are obtained when the design value of $b=1.0$. Thus, the higher values of K ($K=24$) is capable of maintaining a particular P_{fa} in uncertain clutter background. The best performance (least sensitivity to change in b) occurs at $K \geq 18$ for this processor.

6.4 The Detection Performance of the Detector

Fig.(5a) represents the detection performance in homogeneous background of the SO-OS processor as a function of the primary target (SNR in dB), $P_{fa}=10^{-4}$ for window size $M=24$, $K=12$ and the skewness parameter b is variable. Also in the same figures the Non-CFAR and CA-CFAR detection performance curves are plotted. Eq. (3) is used to calculate the P_d of this Processor with the assumption that the noise power has Rayleigh distribution (i.e. $\mu = 1$) and $\alpha_s = \alpha / \mu (1 + \overline{SNR})$. From the displayed results, the detection probability increases by increasing SNR values, and it decreases for more skewed Weibull clutter (b). So, the SNR loss increases as b decreases. For the same parameters and $K=18$ as expected, the SNR loss decreased for this processor as in fig. (6a). Finally, the detection Performance decreases as P_{fa} increases, figs. (5b) to (6b) are plotted at $P_{fa}=10^{-6}$.

Now it is suitable to assume that the noise power (μ) in the reference cells has the same shape of the noise in

the test cell. From fig. (7), it can be seen that the required SNR values for achieving $P_d=0.5$ for SO-OS detector decreases as b decreases. This means that it can be chosen SO detector for more skewed Weibull distribution. For $K=18$, fig. (8), the SNR increases for more skewed Weibull distribution. Smaller values of SNR required achieving a specific P_d at higher values of b . The loss increases for more skewed Weibull distribution. By comparing the two cases ($K=12, 18$), it's clear that the SNR required to achieve $P_d=0.5$, $K=18$ increased for more skewed Weibull distribution. The reason of this case, is the ability of cancellation more spikes signals for $K=12$ than $K=18$.

From the last two curves, the loss increased for SO-OS detector as K increased from 12 to 18. At this case, it can be find a value of the order statistic cell K that gives a constant level of SNR even though the skewness parameter b is variable. Fig. (9) Shows that for $K=14$, the SNR increases by about 0.7 dB as b varies from 2 to 0.1. This means that the best performance of the SO-OS detector is obtained by selecting the order statistic cell (K) near the 60% percentile out of the total cells M , whereas at this value, the SO-OS detector is less sensitive to the shape of the clutter distribution.

6.5 The Performance at Clutter Boundaries

The P_{fa} is determined using Eq. (3) for the detector, with $Q_{E,L}(x)$ as given in

Eq. (12). The threshold multiplier values are calculated previously in section (6.1) for the selected order statistic cell ($K=18$). The false alarm performance of the SO-OS detector is constant and nearest the design value when the number of cells immersed in clutter at either leading or lagging reference window (this curve is not shown). The test sample is assumed to contain a return from clear background region with Rayleigh distributed receiver noise.

The P_{fa} rapidly decreases in the simple CA-CFAR as in Ref. [10]. So, the clutter power has fewer effects on performance of the SO-OS detector family. When more than $M-K$ estimation cells of one of the OS calculators contain clutter, the SO-OS detector selects its power from the second OS calculator, and its P_{fa} is still constant.

When more than M cells immersed in clutter, the test cell responds to this clutter power, the P_{fa} is now higher than the design point ($P_{fa}=10^{-4}$), the false alarm probability increases as shown in fig. (10). The false alarm probability decreases as the number of cells immersed in clutter increases for more than $(2M-K)$ cells and the large false alarm probability can occur at more skewed Weibull distribution.

When all cells lying in clutter, the P_{fa} is now at the design value for Rayleigh distributed clutter. Although, the SO-OS detector has the best detection performance at multiple target situations, this figure shows that its performance degrades rapidly at clutter edges.

Fig. (11) Shows similar performance curve for $K=18$, $R1=6$ and $R2$ is variable. The performance is largely unaffected until $R2 > 6$ estimation cells lie in clutter, this result are obtained when the density function of the test cell responds to Rayleigh distributed receiver noise.

Fig. (12) Shows that the false alarm probability of the detector is still nearest the design value of P_{fa} for Rayleigh distributed clutter until $R2 > 6$. After that, the false alarm probability of the SO-OS detector decreases. These results are plotted in the case of $R1=8$ and $R2$ is variable. Also, the false alarm probability increases as b increases.

6.6 Neyman Pearson Test of the Detector

A simulation of Independent Identically Distributed *Rayleigh* and *Weibull* distributed data [13, 14] is used to test the SO-OS detector for a window size $M=24$, $K=18$, $P_{fa}=10^{-4}$ and the skewness parameter (b) is assumed known a priori.

Using 300 samples, multiple 16 dB point targets have been added at samples 70-105, isolated target at 150 and potentially masked target at 222 by the 15-dB edge at 240 onwards. With reference to fig. (13a):

1. Multiple targets cause masking. The target near the clutter edge is also completely masked and abrupt changes are seen in the threshold.
2. The clutter edge would cause problems for the detector.

It can be seen that the SO-OS detector is capable of overcoming the multiple target problems, Fig. (13b) shows the effect of decreasing the value of the skewness parameter ($b=1$). The threshold level increases as b decreases; also, the fluctuation of the amplitude of the threshold is increases as b decreases for the same value of K , the detection probability decreases as b decreases. For more skewed *Weibull* distribution ($b=0.5$), (this curve is not shown) the required SNR for adjusting P_d at 0.5 should be increases as in figs. (5), and (6) and the best detection performance can be obtained at this value ($b=0.5$).

For $K=12$, $b=2$, approximately, the same detection performance can be obtained as shown in fig. (14a). More skewed *Weibull* distribution has less effects on the performance of this processor and the processor becomes less sensitive to the uncertainty in the clutter distribution (i.e. lower adaptive threshold level than $K=13$) as shown in fig. (14b).

Fig. (15) is plotted at $K=24$ and $b=2$, multiple targets would cause problems, some of these targets undetected. However, the value of $K=M$ cannot be used in practice due to suppression of targets this would give in the presence of multiple targets. In other words, for $K=M$ the noise estimate x will be highest ordered sample which may contain in the interfering target echo with high probability.

If a single extraneous target appears in the reference window, it occupies the highest ranked cell with high probability for the GO-OS and the

conventional OS detector. These increase the overall threshold and may lead to the target miss. If, on the other hand, K is chosen to be less than the maximum value, the OS-CFAR processor will be influenced only slightly for up to $M-K$ interfering targets, as in the past figures. The detector has the best detection performance under these conditions. For more results reference [6, 8] analyzed the performance of GO-OS under Weibull distributed clutter and reference [8] analyzed the performance of CA-CFAR by using FPGA Technology.

7. Conclusions

Limiting the number of false alarms that occur gives robustness to any detection scheme. A multiple targets, where both the power and type of statistics can vary abruptly, the detector are lowered in performance. The SO-OS detector is used to reduce the effect of this problem, with reference to these results, most appealing conclusions are:

- 1) More skewed clutter distribution would require greater threshold increase, and greater concomitant increase in the required SNR.
- 2) The larger values of the order statistic cell K gives the least sensitivity to changes in b .
- 3) The detector will not estimate the clutter mean level exactly as it only uses a finite data sample. The shorter Cell-Averager lengths give higher loss.

- 4) The threshold multiplier values increase as the number of cells M, the order statistic cell K and the skewness parameter b decrease.
- 5) The best performance is obtained by selecting a cell near 75th percentile out of the order statistic calculator for all processors family.
- 6) The detector is found to be relatively insensitive to interference in one of the clutter estimation cells at different skewness parameter.
- 7) The detector is almost not affected by the presence of interfering targets in one of the reference windows; this detector tends to maintain its false alarm rate constant in multiple target environments. However, its behavior against clutter edges is serious.
- 8) A selection of 60% out of the order statistic calculator makes the processor to be less sensitive to the variation in the skewness parameter.

8. References

1. NADAV LEVANON Radar Principles John weley and Sons, USA., (1988).
2. NADAV LEVANON Detection Loss Due to Interfering Targets in IEEE Trans. on AES and Electronic Systems. Vol.AES-24, No.6, March 1988.
3. STEPHEN BLAKE OS-CFAR Theory for Multiple Targets and Nonuniform Clutter IEEE Trans. on AES. and Electronic Systems. Vol. AES-24, No.6, November 1988.

4. Johan Kalvesten Signal Processing and Algorithm Evaluation Tool for Collision Prediction and Crash Sensing Automotive Radars. Dept. of Electrical Eng., Linkoping University-Sweden. 3/6/2004.
5. HILLIP E. PACE, L. LAMOYNE TAYLOR. False Alarm Analysis of the Envelope Detection GO-CFAR Processor IEEE Trans. on AES., vol. 30, No.3, pp.848-864, July 1994.
6. R. RIFKIN Analysis of CFAR Performance in Weibull Clutter IEEE Trans on AES., vol. 30, No.2, pp. 315-327, 1994.
7. SANFORD L. WILSON Two CFAR Algorithms for Interfering Targets and Nonhomogeneous Clutter IEEE Trans. on AES. vol.29, No. 1, pp. 57-72 JANUARY 1993.
8. Ali Jassim Jhaffory Radar Anticlutter Processing By Employing CFAR Techniques. Master Thesis, University of Technology/Iraq. June, 2004.
9. Liu Weixian and Jeffrey S. Fu. A new method for analysis of M-pulses CA-CFAR in weibull background clutter. IEEE International Radar Conference, Alexandria, pp. 509-514, May (7-12) 2000.
10. WEISS M. Analysis of Some Modified Cell- Averaging CFAR Processors in Multiple-Target Situations. IEEE Trans. on AES. vol.18, No.1, pp.102-113. January, 1982.
11. Mohemmed B. EL Mashade Detection analysis of linearly

combined order statistic CFAR algorithms in Nonhomogeneous background environments. Signal Processing 68, pp. 59-71, 1998.

12. Mohamed B. EL Mashade Analysis of adaptive radar systems processing M-Sweeps in target Multiplicity and clutter boundary environments. Signal processing 67, PP.307-329, 1998.
13. GLEN DAVIDSON Doppler Filtering and Detection Strategies for Multifunction Radar. Department of Electrical and Electronic Engineering. University College London October 2000.
14. Richard L. Mitchell Radar Signal Simulation ARTECH HOUSE. USA. 1976.
15. Biao Lhen & Pramod K. Varshney Adaptive CFAR Detection for Clutter Edge Hetrogeneity Using Bayesian Inference. IEEE Trans. on AES. Vol.39, No. 4 October, 2003.
16. SKOLNIK, M. I. Introduction to Radar Systems. McGraw-Hill Book Company, New York, 2001.
17. WEBER P. and Haykin S. Ordered Statistic CFAR Processing for Two Parameter Distributions with variable Skewness IEEE Trans. on AES., vol.,21, No. 6, pp.819-821, November 1985.
18. Herman Rohling. NEW CFAR-PROCESSOR BASED ON ORDERED STATISTIC IEEE International Radar Conference, Alexandria, PP.271-275, May,7-12, 2000.

Smallest Of-Order Statistic-CFAR Analysis in Weibull Clutter

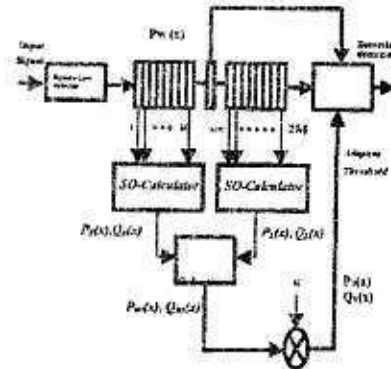


Fig. (1) Block diagram of the SO-OS detector.

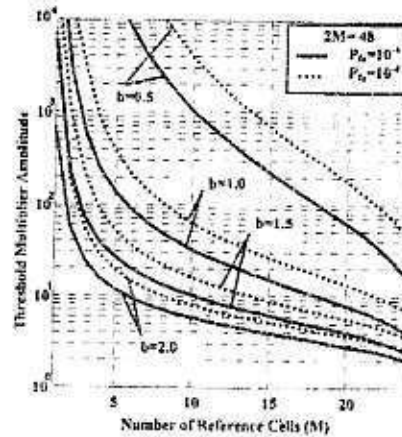


Fig (2) Threshold Multiplier Amplitude for various values of b and P_{fa} .

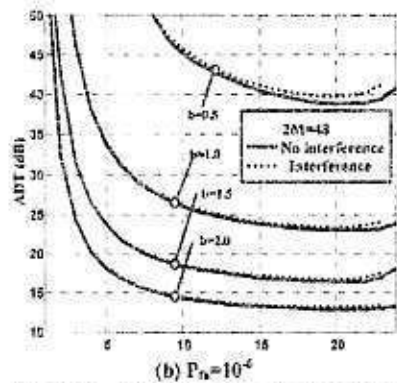
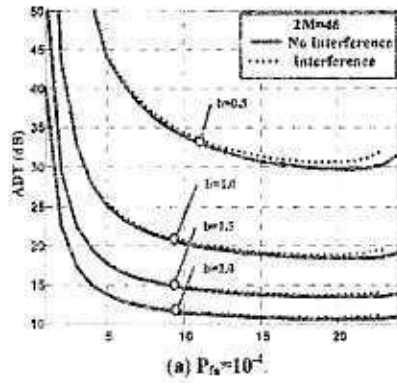


Fig (3) ADT versus the Number of Cells K. (a) $P_{fa}=10^{-4}$, (b) $P_{fa}=10^{-6}$.

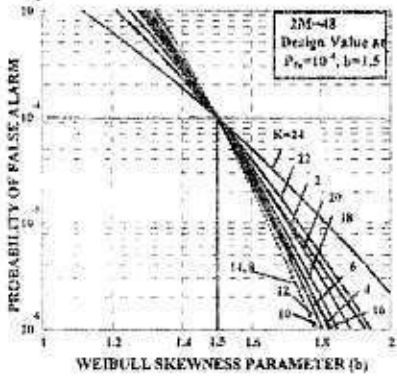


Fig (4) Sensitivity of P_{fa} to b for $P_{fa}=10^{-4}$, $b=1.5$, for the Detector

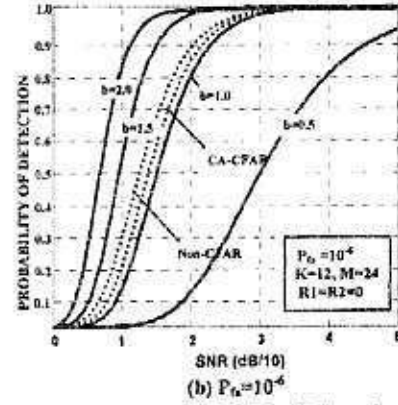
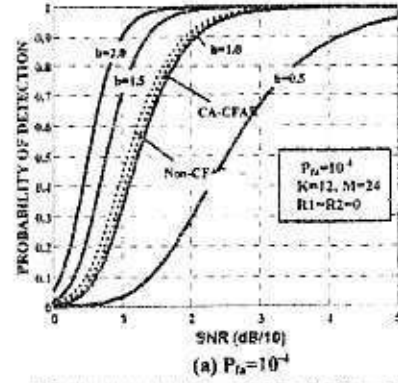


Fig (5) P_d versus SNR for various Weibull skewness parameter b. (a) $P_{fa}10^{-4}$, (b) $P_{fa}=10^{-6}$. (M=24, K=12).

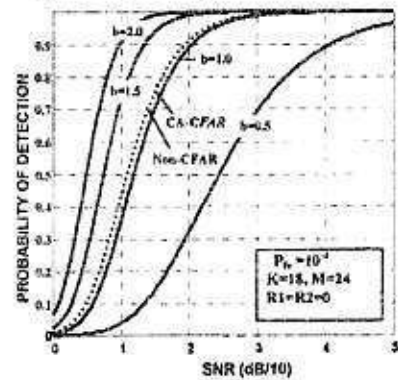


Fig (6) (a) $P_{fa}=10^{-4}$.

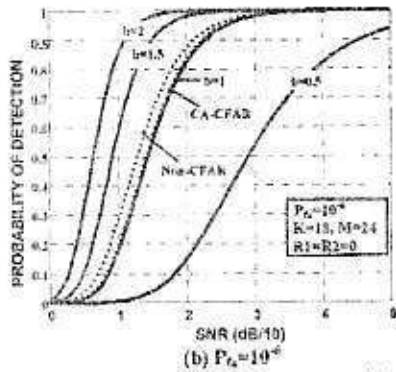


Fig. (6) P_d against SNR with various b (a) $P_{fa}=10^{-4}$, (b) $P_{fa}=10^{-6}$. ($M=24, K=18$).

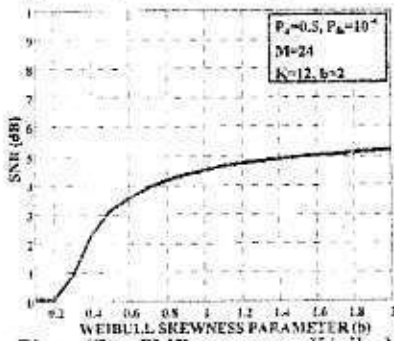


Fig. (7) SNR versus Weibull skewness Parameter b . (Design at $b=2, M=24, K=12, P_d=0.5$)

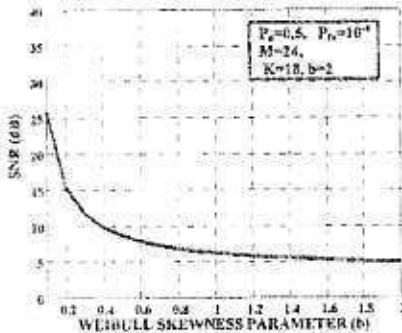


Fig. (8) SNR versus Weibull skewness Parameter b . (Design at $b=2, M=24, K=18, P_d=0.5$)

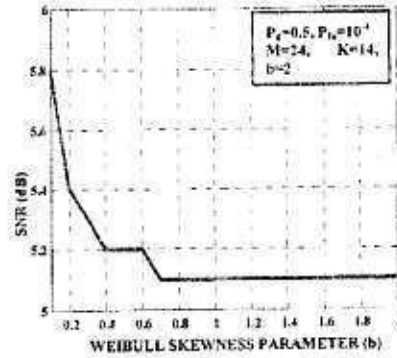


Fig. (9) SNR versus Weibull skewness parameter, (design values at $b=2, M=24, K=14$).

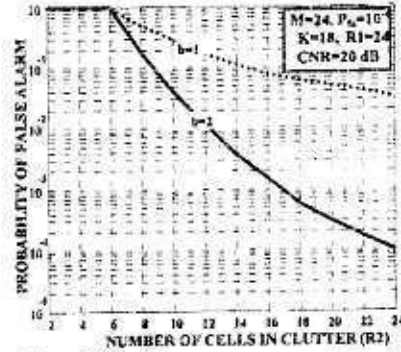


Fig. (10) P_{fa} versus number of cells (R_2) lying in clutter. ($K=18, P_{fa}=10^{-4}, R_1=24, CNR=20$ dB)

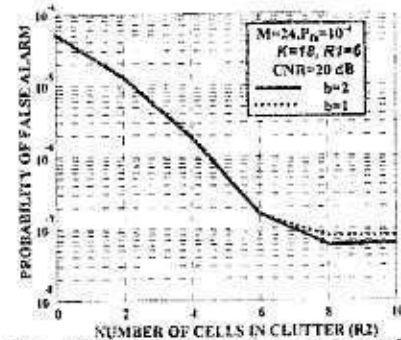


Fig. (11) P_{fa} versus the number of cells (R_2) lying in clutter. ($K=18, R_1=6, P_{fa}=10^{-4}, CNR=20$ dB)

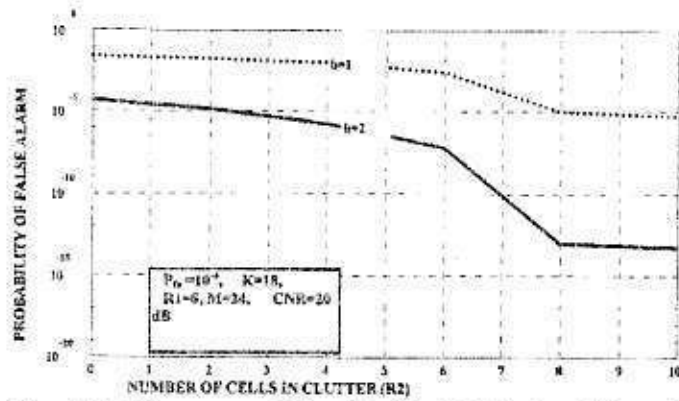


Fig. (12) P_{fa} versus R2. ($K=18$, $R1=8$, $P_{fa}=10^{-4}$ and $CNR=20$ dB)

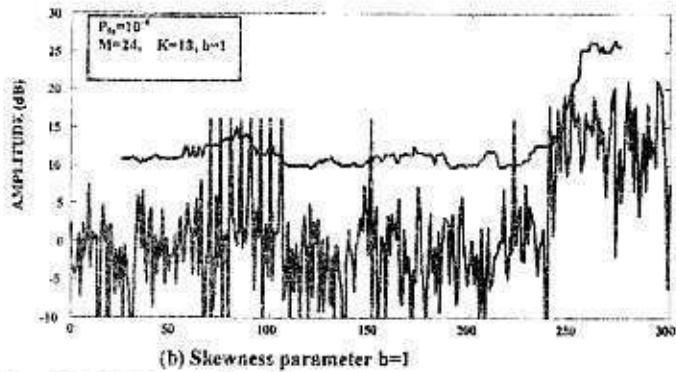
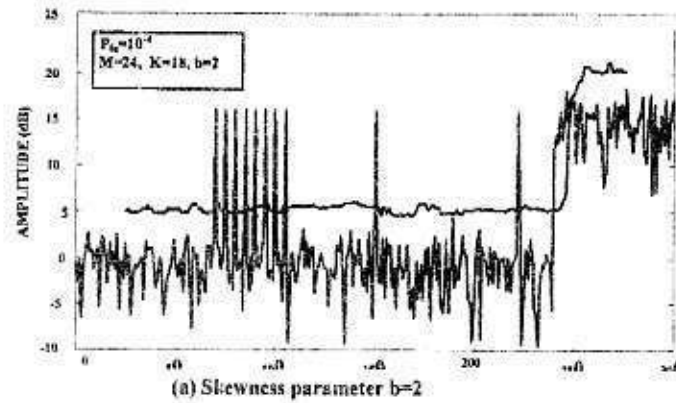


Fig. (13.b) NP test for the detector. (a) $b=2$, (b) $b=1$. ($M=24$, $K=18$, $P_{fa}=10^{-4}$)